

# Permanganate preoxidation affects the formation of disinfection byproducts from algal organic matter

Moshan Chen, Carter A. Rholl, Shane L. Persaud, Zixuan Wang, Zhen He, Kimberly M. Parker\*

Department of Energy, Environmental & Chemical Engineering, Washington University in St. Louis, St. Louis, MO 63130, United States

## ARTICLE INFO

### Keywords:

Harmful algal blooms  
Algal organic matter  
Permanganate preoxidation  
Disinfection byproducts

## ABSTRACT

During harmful algal blooms (HABs), permanganate may be used as a preoxidant to improve drinking water quality by removing algal cells and degrading algal toxins. However, permanganate also lyses algal cells, releasing intracellular algal organic matter (AOM). AOM further reacts with permanganate to alter the abundance of disinfection byproduct (DBP) precursors, which in turn affects DBP formation during disinfection. In this study, we evaluated the impacts of preoxidation by permanganate applied at commonly used doses (i.e., 1–5 mg/L) on DBP generation during chlorination and chloramination of AOM. We found that permanganate preoxidation increased trichloronitromethane (TCNM) formation by up to 3-fold and decreased dichloroacetonitrile (DCAN) formation by up to 40% during chlorination, indicating that permanganate oxidized organic amines in AOM to organic nitro compounds rather than organic nitrile compounds. To test this proposed mechanism, we demonstrated that permanganate oxidized organic amines in known DBP precursors (i.e., tyrosine, tryptophan) to favor the production of TCNM over DCAN during chlorination. Compared to the decreased formation of DCAN during chlorination, permanganate increased DCAN formation by 30–50% during chloramination of AOM. This difference likely arose from monochloramine's ability to react with non-nitrogenous precursors (e.g., organic aldehydes) that formed during permanganate preoxidation of AOM to generate nitrogen-containing intermediates that go on to form DCAN. Our results also showed that permanganate preoxidation favored the formation of dichlorobromomethane (DCBM) over trichloromethane (TCM) during chlorination and chloramination. The increased formation of DBPs, especially nitrogenous DBPs that are more toxic than carbonaceous DBPs, may increase the overall toxicity in finished drinking water when permanganate preoxidation is implemented.

## 1. Introduction

Preoxidation is commonly used during drinking water treatment. Among surface water treatment facilities that implemented preoxidation in the U.S., permanganate was the second most commonly used preoxidant (U.S. EPA, 1999). Permanganate is conventionally used to remove iron and manganese and control the taste and odor of drinking water (U. S. EPA, 1999). Due to its ability to degrade moieties in natural organic matter (NOM) such as olefins, amines, and phenolic compounds (Laszakovits et al., 2020; Perez-Benito, 2009; Waldemer and Tratnyek, 2006), permanganate has also been investigated for its impact on the formation of toxic disinfection byproducts (DBPs) during subsequent disinfection. For example, prior studies reported that permanganate decreased the formation of trihalomethanes (THMs) by 10–20% (He and Ren, 2022; Hidayah and Yeh, 2018; Hu et al., 2018; Rougé et al., 2020a,

2020b) and haloacetonitriles (HANs) by 50–70% (Hu et al., 2018; Rougé et al., 2020a, 2020b) during subsequent chlorination.

Permanganate may also be used as a preoxidant during harmful algal blooms (HABs), which threaten drinking water quality worldwide by causing taste and odor problems and producing toxins (Hallegraeff et al., 2021a, 2021b; Hudnell, 2010; Roberts et al., 2020). During HABs, permanganate preoxidation has been applied to induce aggregation of algal cells for removal by coagulation-flocculation (Chen and Yeh, 2005; Naceradska et al., 2017; Piezner et al., 2021; Qi et al., 2021; Xie et al., 2016), lyse cells to prevent membrane fouling (Fan et al., 2013; Greenstein et al., 2020; Novoa et al., 2021; Piezner et al., 2021; Xie et al., 2013), and degrade certain algal toxins (e.g., microcystins, anatoxin-a) (Rodríguez et al., 2007a, 2007b). However, algal cell lysis caused by permanganate preoxidation also leads to the release of intracellular algal organic matter (AOM) that is a precursor of DBPs (Dong et al.,

\* Corresponding author.

E-mail address: [kmparker@wustl.edu](mailto:kmparker@wustl.edu) (K.M. Parker).

2021; Fang et al., 2010a, 2010b). To date, information regarding the impact of permanganate preoxidation on DBP formation during disinfection of intracellular AOM remains limited. When treating algal cell suspensions, one study showed that permanganate decreased the abundance of trichloromethane (TCM) precursors by up to 40% from extracellular AOM (Shi et al., 2019), while another study found that permanganate preoxidation did not alter DBP formation during subsequent chlorination (Xie et al., 2013). However, the permanganate dosages applied in these studies were too low (<2 mg/L) to lyse algal cells and release intracellular AOM (Fan et al., 2013). The impact of permanganate on intracellular AOM from lysed cells was only investigated by one study, which found that permanganate dosed at 4 mg/L did not alter DBP formation (e.g., TCM, dichloroacetonitrile (DCAN), trichloronitromethane (TCNM)) during subsequent chlorination (Sheng et al., 2022). However, this study reported the impact of permanganate only under a single pair of preoxidant/disinfectant doses (Sheng et al., 2022), which may be insufficient to account for preoxidant effects that depend on the doses of preoxidant and disinfectant (Hua and Reckhow, 2008; Rougé et al., 2020a, 2020b).

Whereas preoxidants tend to decrease DBP formation from NOM, preoxidants other than permanganate have been found to increase the formation of DBPs from AOM. For example, preoxidation using chlorine dioxide decreased the formation of TCM by 10% and DCAN by 60% during chlorination of NOM (Yang et al., 2013), but increased the formation of these DBPs during chlorination of intracellular AOM (i.e., by 60% for TCM, 50% for DCAN) (Sheng et al., 2022). Like chlorine dioxide, ozone typically decreased THM formation by 20–50% during chlorination of NOM (Jiang et al., 2016, 2019; Rougé et al., 2020b), but increased THM formation by 30–70% during chlorination of AOM (Chien et al., 2018; Sheng et al., 2022; Zhou et al., 2015; Zhu et al., 2015). The increased formation of DBPs from AOM may result from specific changes made by the preoxidants to AOM properties (e.g., decreasing its molecular weight, aromaticity, or hydrophobicity) (Dong et al., 2021; Sheng et al., 2022; Zhou et al., 2015). In addition, some preoxidants react with specific moieties from AOM to generate DBPs. For example, organic amines, which are more abundant in AOM than NOM (Dong et al., 2021; Fang et al., 2010b), were oxidized by ozone to generate precursors of TCNM (McCurry et al., 2016), which could contribute to a greater extent of increase in the formation of TCNM by preozonation observed from AOM (i.e., 5- to 100-fold) than NOM (i.e., 2- to 8-fold) (Chien et al., 2018; Jiang et al., 2016, 2019; Sheng et al., 2022; Zhou et al., 2015; Zhu et al., 2015).

In this study, we hypothesized that permanganate preoxidation increases DBP formation during disinfection of AOM in contrast to NOM, which was included as a control throughout the study. Using AOM derived from cultivated *Microcystis aeruginosa*, we first tested the effects of permanganate on DBP formation during chlorination of AOM and linked some of these effects to the reaction of permanganate with specific moieties in AOM (i.e., organic amines). We next extended our work to investigate the impact of permanganate on DBP formation during chloramination of AOM, which we hypothesized would differ from chlorination due to monochloramine acting as a weaker oxidant that can also participate in unique reactions that generate new DBP precursors, particularly for nitrogenous DBPs (Fang et al., 2010b; Pedersen et al., 1999; Shah and Mitch, 2012). Finally, we evaluated the impact of permanganate preoxidation on calculated toxicity associated with DBP formation (Szczuka et al., 2017; Wagner and Plewa, 2017; Zeng et al., 2016). In contrast to prior findings under limited conditions (Sheng et al., 2022), our work demonstrated that permanganate preoxidation increased the formation of some DBPs specifically from AOM under relevant doses of permanganate and disinfectant.

## 2. Materials and methods

### 2.1. Chemicals and reagents

All chemicals (Table S1) were used as received. Oxidant solutions were prepared in Milli-Q water as described in Text S1. We obtained AOM from *Microcystis aeruginosa* following the method described in Text S2. For experiments, AOM was added to Milli-Q water at a concentration of 5 mg-C/L, which is approximately equivalent to the concentration of AOM that would be released by algal cells present at 10<sup>6</sup> cells/mL (Fang et al., 2010a; Xie et al., 2013). We obtained NOM from natural water samples that were collected from the Mississippi River at a location near the Chain of Rocks Water Treatment Plant in St. Louis, Missouri, where no HAB was reported at the time of collection. The water samples were filtered through 0.7 µm glass fiber filters (Fisher) that were pre-baked in an oven at 450 °C for 4 h. These water samples were directly used for experiments requiring NOM and contained total organic carbon (TOC) measured to be 3 mg-C/L. Water quality parameters including TOC, specific UV absorbance at 254 nm (SUVA<sub>254nm</sub>), and concentrations of inorganic ions were measured for solutions containing AOM and NOM as described in Text S3 and are shown in Table S2. All solutions containing either AOM or NOM were stored at 4 °C.

### 2.2. Experimental procedure

Experiments were conducted to measure the concentrations of DBPs generated during permanganate preoxidation and disinfection of AOM and NOM. All solutions contained 5 mg-C/L AOM or 3 mg-C/L NOM, 10 mM phosphate buffer (pH 7), and permanganate at concentrations commonly used during preoxidation (i.e., 1–5 mg/L as potassium permanganate, KMnO<sub>4</sub>) (Dong et al., 2021; Piezner et al., 2021; U.S. EPA, 1999). The solutions were prepared in 40 mL amber glass vials that were headspace-free and reacted at room temperature in the dark for 3 d to allow sufficient time for reactions between permanganate and moieties in organic matter (Laszakovits et al., 2022). After 3 d, residual permanganate in solutions was measured. To terminate the reaction, a quencher was applied at >10-fold molar excess relative to permanganate concentrations in a 100 µL aliquot. Sodium thiosulfate was used to quench permanganate in an early experiment (i.e., Fig. 1a-d), but was replaced with ascorbic acid in all later experiments including Fig. 3a-d that replicated identical experimental conditions to achieve the same results after permanganate preoxidation alone. These quenched solutions were extracted into methyl tert-butyl ether (MtBE) within 30 min as described in Text S4. Then, DBP concentrations in the MtBE extracts were analyzed to determine the amount generated during permanganate preoxidation.

To a separate set of unquenched solutions after permanganate preoxidation, small volumes (i.e., <100 µL) of disinfectant stock solutions were added into each vial to achieve a targeted concentration (i.e., 15 mg/L chlorine or 4 mg/L monochloramine as chlorine, Cl<sub>2</sub>) for disinfection carried out over 3 d. The disinfection time was selected to align with other studies investigating DBP formation from AOM (Fang et al., 2010a, 2010b; Shi et al., 2019; Xie et al., 2013), while oxidant concentrations were selected to maintain residuals after the disinfection period (Figure S1). Subsequently, solutions were quenched with ascorbic acid, extracted, and analyzed for DBP concentrations generated during disinfection.

For experiments investigating the impact of permanganate preoxidation on DBP formation during chlorination of model organic amines (i.e., tyrosine and tryptophan), 3.2 mg-C/L tyrosine or 4.0 mg-C/L tryptophan (i.e., 30 µM) were treated with 1–50 mg/L permanganate (as KMnO<sub>4</sub>, i.e., 6–320 µM) during preoxidation. These concentrations spanned values above and below permanganate demand in these experiments. After 3 d, solutions were measured for residual permanganate concentrations or treated with chlorine as described above.

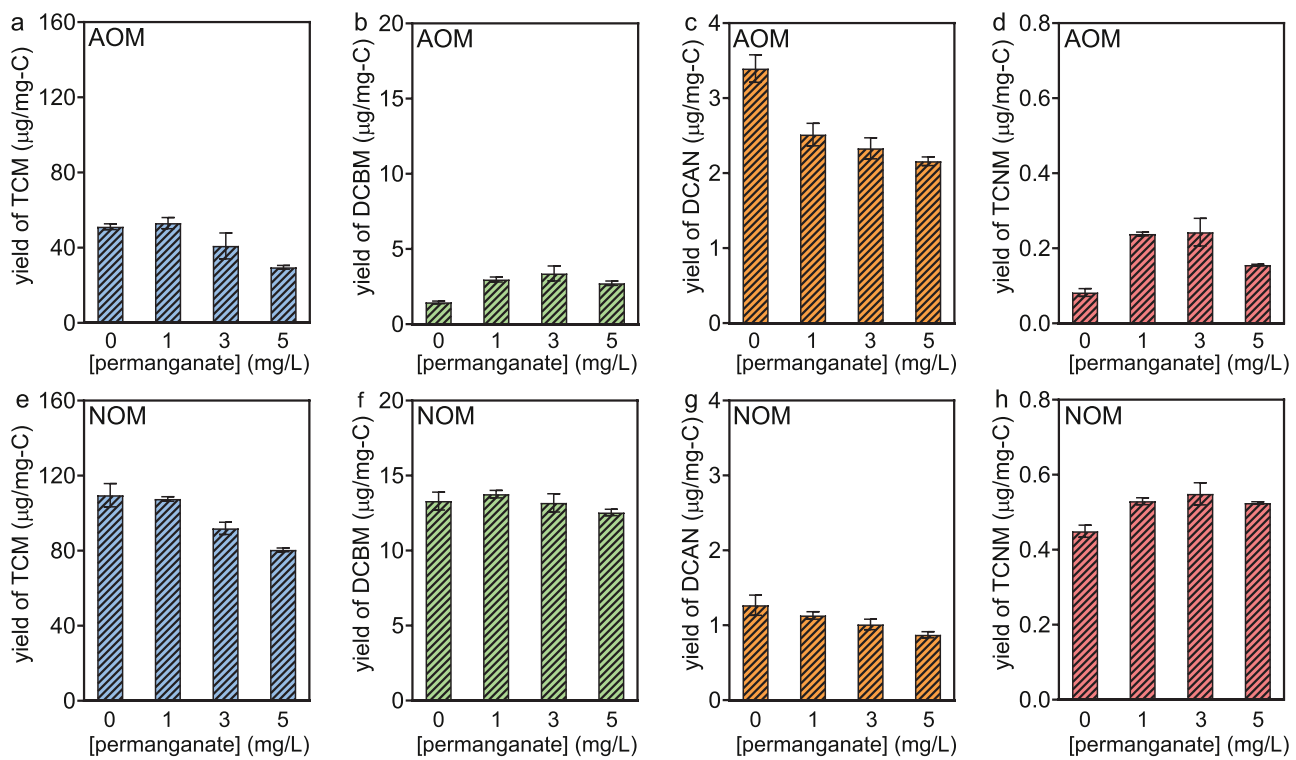


**Fig. 1.** Formation of trichloromethane (TCM), dichlorobromomethane (DCBM), dichloroacetonitrile (DCAN), and trichloronitromethane (TCNM) during preoxidation by permanganate (as  $\text{KMnO}_4$ ) for 3 d followed by chlorination of AOM (a-d) or NOM (e-h) for 3 d. All solutions were prepared in headspace-free amber vials initially containing 5 mg-C/L AOM (a-d) or 3 mg-C/L NOM (e-h), permanganate at the indicated concentration, and 10 mM phosphate buffer (pH 7). After 3 d, 15 mg/L chlorine (as  $\text{Cl}_2$ ) was added as the disinfectant to all solutions. DBP yields after permanganate preoxidation without chlorination were below the method detection limits (i.e., 0.1  $\mu\text{g}/\text{L}$ : 0.02  $\mu\text{g}/\text{mg-C}$  for AOM, 0.03  $\mu\text{g}/\text{mg-C}$  for NOM). Error bars represent the standard deviation of triplicate experiments.

### 2.3. Analytical procedures

Concentrations of residual oxidants were measured as described in Text S5. Residual chlorine and monochloramine concentrations were measured after disinfection for 3 d without preoxidation (Figure S1). Residual permanganate concentrations were measured after preoxidation of AOM and NOM (Figure S2) and model amino acids (Figure S3), each for 3 d.

Four THMs (i.e., TCM, dichlorobromomethane (DCBM), dibromochloromethane (DBCM), tribromomethane (TBM)), three haloacetonitriles (i.e., DCAN, bromochloroacetonitrile (BCAN), dibromoacetonitrile (DBAN)), and TCNM were measured on gas chromatography-mass spectrometry (GC-MS, Text S4). In all of our experiments, we only detected four of these DBPs above the levels of their method detection limit: TCM (0.1  $\mu\text{g}/\text{L}$ ), DCBM (0.1  $\mu\text{g}/\text{L}$ ), DCAN (0.1  $\mu\text{g}/\text{L}$ ), and TCNM (0.1  $\mu\text{g}/\text{L}$ ). All other measured DBPs never occurred at concentrations above the levels of their detection limit: DBCM (0.1  $\mu\text{g}/\text{L}$ ), TBM (0.1  $\mu\text{g}/\text{L}$ ), BCAN (0.2  $\mu\text{g}/\text{L}$ ), DBAN (0.1  $\mu\text{g}/\text{L}$ ).

The toxicity associated with detected DBPs was calculated by dividing the molar concentration of each DBP by their corresponding LC<sub>50</sub> cytotoxicity values (i.e., the DBP concentration that results in 50% reduction in growth of Chinese hamster ovary cells compared to the untreated control), which facilitates quantitative comparison of DBP toxicities determined using a common assay (Szczuka et al., 2017; Wagner and Plewa, 2017; Zeng et al., 2016). The calculated toxicity aggregates the contributions of several DBPs measured on a consistent basis, though notably it does not account for toxicity contributed by other DBPs occurring below method detect limits nor excluded from the analytical method (McKenna et al., 2020).

### 2.4. Statistical analysis

All experiments were conducted in triplicate. Error bars represent the standard deviations of the data obtained from triplicate experiments. The significance of differences between DBP formation with and without preoxidation was assessed by two-tail t-tests in GraphPad Prism with a confidence level set to be  $\leq 0.05$ .

## 3. Results and discussion

### 3.1. DBP formation from disinfection without preoxidation

Before investigating the impact of preoxidation on the abundance of DBP precursors, we first measured the production of DBPs from AOM during chlorination or chloramination in the absence of preoxidation as a control. During chlorination and chloramination, we found that TCM, DCBM, DCAN, and TCNM were generated from AOM, while other four DBPs included in our method were below their detection limits (Table S3). The yields of measurable DBPs ( $\mu\text{g}$  per mg-C) were comparable to those reported in previous literature during chlorination of AOM, indicating that our AOM behaved similarly to AOM used in other studies (Table S4) (Fang et al., 2010a, 2010b; Gu et al., 2020; Hua et al., 2017; Kralles et al., 2020; Li et al., 2012; Plummer and Edzwald, 2001; Shi et al., 2019; Wert and Rosario-Ortiz, 2013; Xie et al., 2013; Yang et al., 2011; Zhang et al., 2014, 2016; Zhou et al., 2015, 2014; Zhu et al., 2015). Similarly, our results showed that the yields of TCM, DCAN, and TCNM from chloramination of AOM were also comparable to the previously reported ranges from AOM (Table S5) (Fang et al., 2010b; Gu et al., 2020; Yang et al., 2011; Zhu et al., 2015). Among the four DBPs that formed at measurable quantities, we found that DCBM formed at the lowest yield, which was 30- to 80-fold lower than the previously reported yields (Table S5) obtained from AOM samples amended with

bromide (i.e., 0.05–1 mg/L) (Gu et al., 2020).

To enable a comparison between AOM and NOM, we also measured the production of DBPs from NOM during chlorination and chloramination. Similar to AOM, only four among eight DBPs (i.e., TCM, DCBM, DCAN, TCNM) were detectable during disinfection of NOM. Similar to the yields of DBPs from AOM, the yields of these four DBPs from NOM were comparable to previously reported ranges during chlorination (Table S4) (Fang et al., 2010a, 2010b; Gallard and Von Gunten, 2002; Hua et al., 2015; Huang et al., 2017; Jiang et al., 2019; Liang and Singer, 2003; Lu et al., 2009; Rougé et al., 2020b; Xu et al., 2011; Yang et al., 2013, 2011; Zhang et al., 2020) and chloramination (Table S5) (Fang et al., 2010b; Hua et al., 2015; Huang et al., 2017; Jiang et al., 2019; Lu et al., 2009; Yang et al., 2013). Compared to AOM, NOM yielded more carbonaceous DBPs (C-DBPs) during chlorination (i.e., ~2-fold more TCM and ~10-fold more DCBM, Table S4) and chloramination (i.e., ~30-fold more DCBM, Table S5). The higher yields of C-DBPs, particularly TCM, may be attributed to a higher content of aromatic organic carbon from NOM than AOM (Fang et al., 2010b) that is correlated with a higher value of SUVA<sub>254 nm</sub> (Reckhow et al., 1990) from NOM (i.e., 3.5 L/(mg-C·m)) than AOM (i.e., 1.0 L/(mg-C·m), Table S2). NOM also yielded ~3-fold less DCAN and ~5-fold more TCNM than AOM during chlorination (Table S4). The total N-DBP yield (dominated by DCAN) from NOM was less than from AOM, likely because AOM has been reported to have ~20-fold higher abundance of organic nitrogen relative to organic carbon than NOM (Fang et al., 2010b).

### 3.2. DBP formation from permanganate preoxidation followed by chlorination

To investigate the effects of permanganate preoxidation on the abundance of DBP precursors from AOM and NOM, we next added 1–5 mg/L permanganate before chlorination. Measured DBPs were never detected after permanganate preoxidation of AOM (Fig. 1a-d) and NOM (Fig. 1e-h) for 3 d. Therefore, the effects of permanganate on DBP formation after chlorination were entirely attributable to the effects of permanganate on precursors that subsequently reacted with chlorine rather than DBP formed from permanganate itself.

When we used 1 mg/L initial permanganate during preoxidation, the production of TCM during subsequent chlorination of AOM was comparable to the control (Fig. 1a). When the concentration of permanganate was increased to 3 and 5 mg/L, the yield of TCM decreased by 20 ±10% and 42±4%, respectively, relative to the control (Fig. 1a). Compared to AOM, we found similar effects of permanganate preoxidation on TCM yield from NOM (Fig. 1e). Our results showed marginally greater decreases in TCM yield from AOM and NOM than the slight decrease reported in a prior report (i.e., by <5%) during chlorination of NOM under similar experimental conditions (Rougué et al., 2020b). The decreased TCM formation indicates that permanganate degrades TCM precursors from AOM and NOM.

In addition to TCM, DCBM was also detected after chlorination of both AOM and NOM (Fig. 1b,f). Although we found low concentrations of bromide in solutions containing AOM (i.e., <0.01 mg/L, below the detection limit) and NOM (i.e., 0.02 mg/L) (Table S2), oxidation of trace bromide may still have led to the formation of hypobromous acid (Heeb et al., 2014; Kumar and Margerum, 1987) or other brominating oxidants (Broadwater et al., 2018; Sivey et al., 2015, 2013) that react with organic matter to generate brominated DBPs like DCBM. In contrast to the decreased yield of TCM after permanganate preoxidation (Fig. 1a,e), the yield of DCBM during chlorination was either unchanged or increased upon preoxidation of NOM or AOM, respectively (Fig. 1b, f). While the exact causes of the different effects of permanganate preoxidation on DCBM formation relative to TCM are unknown, it is possible that permanganate reacts differently with their respective precursors, which are somewhat distinct. For example, DBPs with more brominated substituents were found to be preferentially generated from more hydrophilic organic matter fractions relative to their chlorinated analogues

(Hua and Reckhow, 2007; Liang and Singer, 2003), suggesting possible differences in the precursors of TCM and DCBM alter the effects of preoxidation on their eventual formation.

We next investigated the impact of permanganate preoxidation on the formation of N-DBPs including DCAN. We found that preoxidation by 1–5 mg/L permanganate decreased the yield of DCAN from AOM by up to 40% relative to the control (Fig. 1c). Similarly, permanganate decreased the yield of DCAN from NOM (Fig. 1g). The decrease in DCAN yield from NOM was comparable to the previously reported decrease during chlorination of NOM (i.e., by ~40%) under similar experimental conditions (Rougué et al., 2020b). Our results indicate that, like its impact on DCAN precursors from NOM, permanganate also degrades DCAN precursors from AOM during preoxidation.

Although permanganate preoxidation decreased the formation of DCAN, it increased the formation of the other detected N-DBP, TCNM, from both AOM and NOM. Specifically, permanganate at 1 and 3 mg/L increased the yield of TCNM from AOM by ~3-fold relative to the control (Fig. 1d). A moderate decrease in TCNM yield was observed when permanganate was increased to 5 mg/L (Fig. 1d), possibly due to further oxidation of TCNM precursors similar to TCM precursors (Fig. 1a). Compared to the large increase in TCNM yield from AOM, permanganate preoxidation only slightly increased the yield from NOM by ~20% relative to the control (Fig. 1h). The greater increase in TCNM yield from AOM than NOM may be explained by the higher amount of organic nitrogen in AOM than NOM (Fang et al., 2010b), which makes AOM more susceptible to react with permanganate to form TCNM precursors.

The different effects of permanganate on the formation of DCAN and TCNM from AOM in our experiments might result from the fact that they were both proposed to be generated from organic amine precursors (e.g., amino acids, proteins) during the chlorination of AOM (Fang et al., 2010b). One key difference in their formation mechanisms is the transformation from organic amines to organic nitrile compounds (i.e., R-C≡N) or organic nitro compounds (i.e., R-NO<sub>2</sub>), which leads to the formation of DCAN or TCNM, respectively (Fang et al., 2010b; Laszakovits et al., 2022; Shah and Mitch, 2012). We hypothesized that permanganate oxidizes organic amines from AOM to form organic nitro compounds (Scheme 1, step 1) (Laszakovits et al., 2022; Li et al., 2021; Wei, 1965), which contributes to the increased formation of TCNM during subsequent chlorination (step 2) (Fang et al., 2010b; Shah and Mitch, 2012). However, oxidation of amines to nitro groups may reduce the abundance of precursors that go on to form organic nitrile compounds (step 3) and subsequently DCAN (step 4) during chlorination (Fang et al., 2010b; Shah and Mitch, 2012).

To test our hypothesis regarding the effect of permanganate preoxidation on N-DBP precursors from organic amines, we measured the formation of both DCAN and TCNM from two known amine-containing precursors, namely, the amino acids tyrosine and tryptophan (Jia et al., 2016; Yang et al., 2012). Notably, even though the carbon-based concentration of 30 μM solutions of tyrosine and tryptophan were similar to AOM and NOM (i.e., 3–4 mg-C/L relative to 3–5 mg-C/L, respectively), the permanganate demands of the model compounds were much higher (Figure S3), likely due to a greater abundance of reactive sites present relative to carbon mass. Consequently, for this mechanistic experiment, permanganate was applied at both a lower concentration range (1–5 mg/L) – corresponding to that used for AOM and NOM experiments – and a higher concentration range (10–50 mg/L) – spanning the measured permanganate demand of 3.2 mg-C/L tyrosine (i.e., 27.6 ± 0.7 mg/L) and 4.0 mg-C/L tryptophan (i.e., 41.2 ± 0.4 mg/L) (Figure S3). The greater permanganate demand by tryptophan than tyrosine likely resulted from permanganate selectively reacting with the indoleamine in tryptophan (Fig. 2) (Laszakovits et al., 2022), though tyrosine and tryptophan exert similar demands for other common preoxidants (e.g., chlorine, ozone) (Hureki et al., 1998; R. Wang et al., 2020).

The effect of permanganate preoxidation on DCAN and TCNM

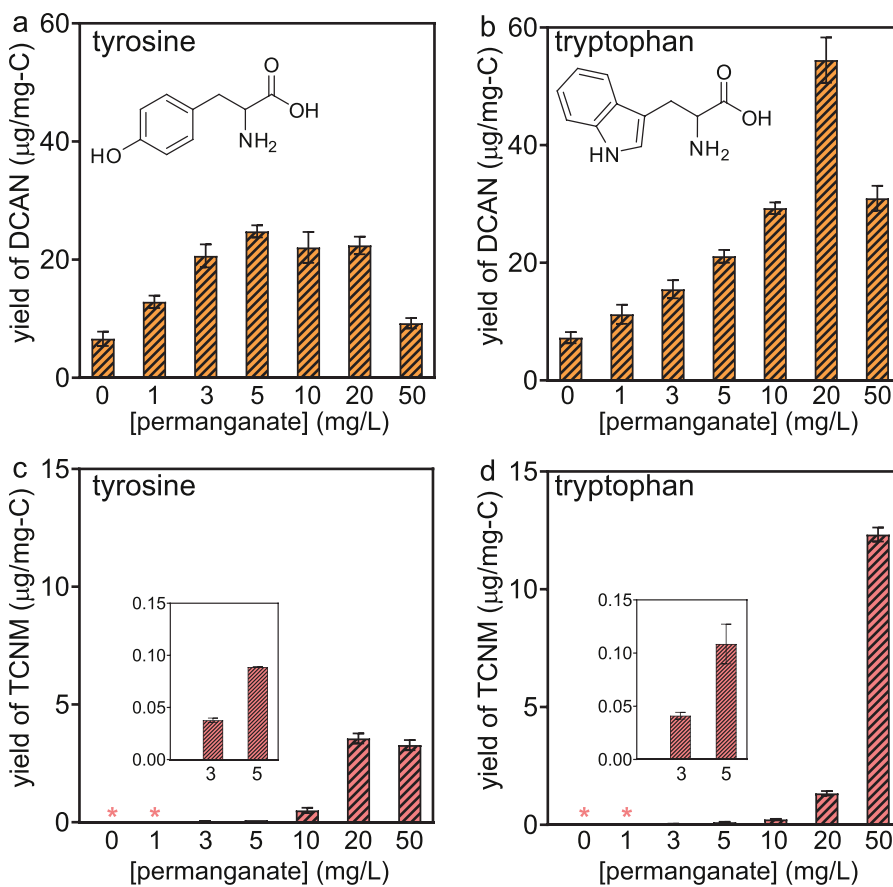


**Fig. 2.** Formation of dichloroacetonitrile (DCAN) and trichloronitromethane (TCNM) during preoxidation by permanganate (as  $\text{KMnO}_4$ ) for 3 d followed by chlorination of tyrosine (a,c) or tryptophan (b,d) for 3 d. All solutions were prepared in headspace-free amber vials initially containing 3.2 mg-C/L tyrosine (a,c) or 4.0 mg-C/L tryptophan (b,d) (i.e., both 30  $\mu\text{M}$ ), permanganate at the indicated concentration, and 10 mM phosphate buffer (pH 7). After 3 d, 15 mg/L chlorine (as  $\text{Cl}_2$ ) was added as the disinfectant to all solutions. DBP yields after permanganate preoxidation without chlorination were below the method detection limits (i.e., 0.1  $\mu\text{g/L}$ :  $\sim 0.031 \mu\text{g/mg-C}$  for tyrosine,  $\sim 0.025 \mu\text{g/mg-C}$  for tryptophan). The asterisks (\*) in (c) and (d) indicate TCNM occurred at concentrations below its method detection limit. Error bars represent the standard deviation of triplicate experiments.

formation during chlorination of tyrosine and tryptophan differed when permanganate was below or above the permanganate demand of the amino acid precursors. In all cases where permanganate was applied below the permanganate demand of the amino acids (i.e., 20 mg/L or lower), DCAN yield tended to increase with increasing permanganate doses (Fig. 2a,b). Notably, whereas DCAN yield from tryptophan increased continuously as the permanganate dose was increased from 1 to 20 mg/L (Fig. 2b), the DCAN yield from tyrosine plateaued when permanganate dose was increased from 5 to 20 mg/L (Fig. 2a), which may be related to tryptophan's greater permanganate demand relative to tyrosine (Figure S3). When permanganate dose was applied in excess of the demand (i.e., when permanganate dose was increased from 20 to 50 mg/L), DCAN yield from both tyrosine and tryptophan decreased. In contrast to the dose-dependent effect of permanganate on DCAN yield, TCNM increased consistently with increasing permanganate doses above 3 mg/L (Fig. 2c,d). The greatest increase in TCNM occurred when permanganate dose approached or exceeded the demand of the two amino acids.

Overall, our results collected using amino acids suggest that the effects of permanganate on DCAN and TCNM formation from organic amine precursors depends on the amount of permanganate applied relative to the demand exerted by the precursors. We found that higher doses of permanganate decreased DCAN formation and increased TCNM, but only under the condition where permanganate was applied in excess of the precursor's demand. Notably, this condition was met during our experiments using AOM, wherein all permanganate doses (1–5 mg/L) exceeded the demand (i.e.,  $< 1 \text{ mg/L}$ , Figure S2). At lower permanganate doses, DCAN formation from amino acids increased, which suggests that partially oxidized intermediates generated from the reaction of the amino acids with permanganate serve as better precursors for DCAN than the parent molecules. This finding is in stark contrast to a prior study that reported preoxidation of amino acids by

permanganate at doses ranging from 1 to 5 mg/L resulted in decreased formation of both DCAN and TCNM (Wang et al., 2020). A possible cause for this difference is the elevated chlorine dose (i.e., 213 mg/L as  $\text{Cl}_2$ ) employed by the prior study (Wang et al., 2020), which may have sufficiently oxidized the amino acids in the absence of permanganate to mask the effect of preoxidation on N-DBP precursors detectable under the more relevant conditions applied in our experiments using AOM. Together, results from both our study and the prior study point to important effects of both preoxidant and disinfectant concentrations in determining the overall effect of preoxidation on DBP formation.

### 3.3. DBP formation from permanganate preoxidation followed by chloramination

We next investigated the impact of permanganate on the abundance of DBP precursors from AOM when monochloramine was applied during disinfection. We hypothesized that DBP formation during chloramination is more sensitive to permanganate preoxidation because monochloramine is a weaker oxidant than chlorine and therefore reacts with a smaller pool of precursors. The ability of monochloramine to react with fewer DBP precursors in both AOM and NOM relative to chlorine was further evidenced by both lower DBP yields (i.e., Fig. 3 vs. Fig. 1) and disinfectant demand (Figure S4). This difference between the reactivities of monochloramine and chlorine therefore may translate to differences in the effect of permanganate preoxidation on ultimate DBP formation.

Whereas TCM formation during chlorination decreased after preoxidation by higher levels of permanganate (Fig. 1a), the impact of permanganate on TCM formation during chloramination of AOM varied depending on permanganate concentration (Fig. 3a). Surprisingly, at the lowest dose of permanganate (i.e., 1 mg/L), TCM yield increased by 70% (Fig. 3a), which suggests that permanganate at a relatively low

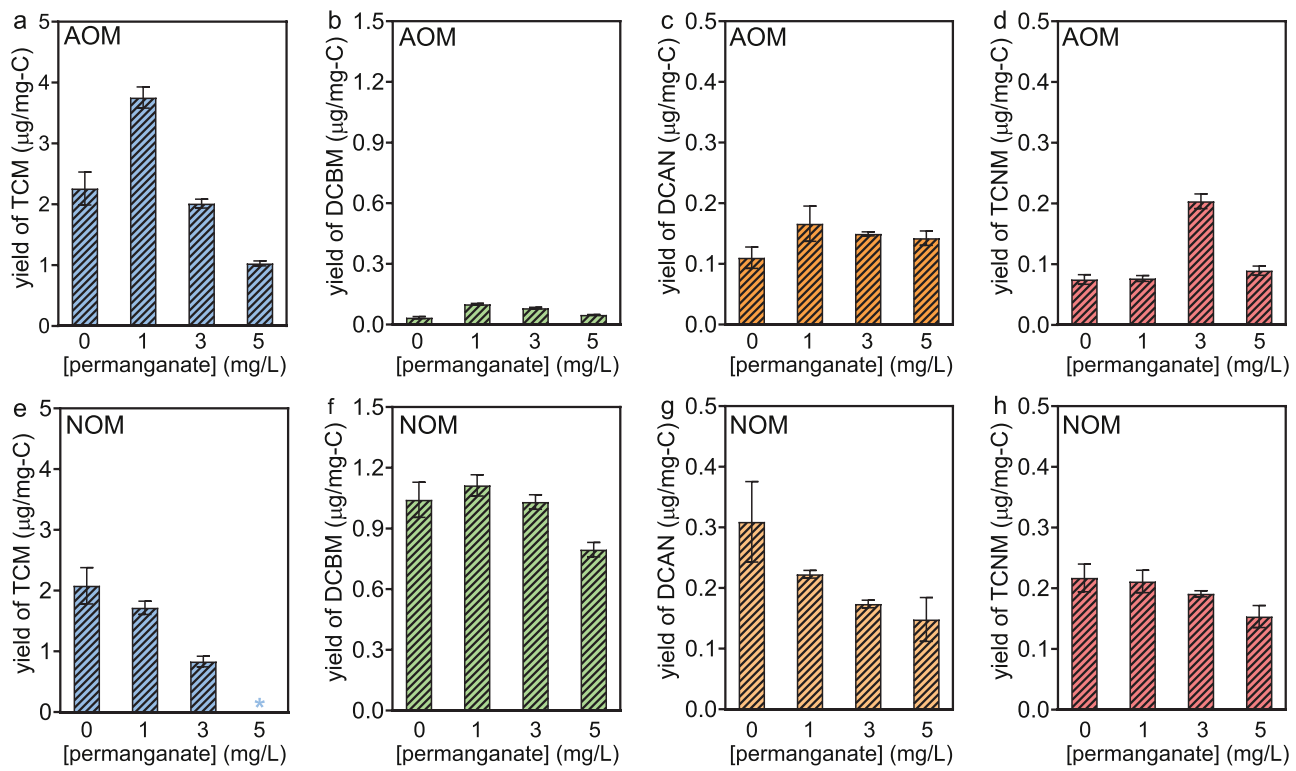


**Fig. 3.** Formation of trichloromethane (TCM), dichlorobromomethane (DCBM), dichloroacetonitrile (DCAN), and trichloronitromethane (TCNM) during preoxidation by permanganate (as  $\text{KMnO}_4$ ) for 3 d followed by chloramination of AOM (a-d) or NOM (e-h) for 3 d. All solutions were prepared in headspace-free amber vials initially containing 5 mg-C/L AOM (a-d) or 3 mg-C/L NOM (e-h), permanganate at the indicated concentration, and 10 mM phosphate buffer (pH 7). After 3 d, 4 mg/L monochloramine (as  $\text{Cl}_2$ ) was added as the disinfectant to all solutions. DBP yields after permanganate preoxidation without chloramination were below the method detection limits (i.e., 0.1  $\mu\text{g}/\text{L}$ : 0.02  $\mu\text{g}/\text{mg-C}$  for AOM, 0.03  $\mu\text{g}/\text{mg-C}$  for NOM), except TCM that was yielded at  $0.029 \pm 0.007$  and  $0.04 \pm 0.01 \mu\text{g}/\text{mg-C}$  after preoxidation of AOM by 1 and 3 mg/L permanganate, respectively. The asterisk (\*) in (e) indicates TCM occurred at concentrations below its method detection limit. Error bars represent the standard deviation of triplicate experiments.

concentration reacts with AOM to form TCM precursors that more readily react with monochloramine but not chlorine. However, at higher permanganate doses (i.e., 3 and 5 mg/L), TCM yield decreased down to 50% of the control (Fig. 3a), in closer alignment to decreasing yields observed from NOM upon permanganate preoxidation (Fig. 3e). Notably, TCM yield during chloramination of NOM was highly sensitive to permanganate preoxidation, decreasing to below the method detection limit when permanganate was applied at its highest dose (Fig. 3e). Consequently, permanganate preoxidation appears capable of dramatically eliminating the relatively small pool of TCM precursors from NOM that react with monochloramine, but is less effective at degrading TCM precursors from AOM.

In contrast to TCM, the effects of permanganate preoxidation on the formation of DCBM during chloramination of both AOM (Fig. 3b) and NOM (Fig. 3f) were more similar to the effect observed during chlorination (Fig. 1b,f). We again observed that permanganate preoxidation increased the yield of DCBM during chloramination of AOM, in this case by up to ~3-fold (Fig. 3b), while the yield of DCAN during chloramination of NOM remained unchanged or slightly decreased (Fig. 3f). As observed for TCM, the greatest increase in DCBM yield from AOM was found at the lowest permanganate dose (i.e., 1 mg/L); however, DCBM yields remained above the control even at higher permanganate doses. Together, our results from both chlorination and chloramination suggest that AOM, but not NOM, specifically reacts with permanganate to generate DCBM precursors.

Another key difference between chlorination and chloramination was observed when comparing the impact of permanganate on DCAN formation. Unlike the decreased yield of DCAN during chlorination of both AOM and NOM (Fig. 1c,g), the impact of permanganate preoxidation on DCAN yield during chloramination differed between AOM

and NOM (Fig. 3c,g). While we still found a decreased yield of DCAN during chloramination of NOM (i.e., up to 50%, Fig. 3g), permanganate preoxidation surprisingly increased the yield of DCAN during chloramination of AOM (i.e., by 30–50%, Fig. 3c). When considering DCAN formation during chlorination, we proposed that permanganate preoxidation shifts N-DBP formation from organic amines towards TCNM instead of DCAN (Fig. 2), possibly due to oxidation of amines to nitro compounds (Scheme 1). While permanganate may still convert organic amines to organic nitro compounds over organic nitrile compounds before chloramination, monochloramine serves as an additional source of nitrogen for DCAN formation (Fang et al., 2010b; Pedersen et al., 1999; Shah and Mitch, 2012). In this case, permanganate may have reacted with AOM to form other DCAN precursors such as organic aldehydes (Li et al., 2021; Rawalay and Shechter, 1967; Shaabani et al., 2005; Shechter and Rawalay, 1964; Wei, 1965). The nucleophilic attack of monochloramine on the aldehyde leads to the formation of organic nitrile compounds (Fang et al., 2010b; Pedersen et al., 1999; Shah and Mitch, 2012), which in turn increase the formation of DCAN during chloramination (Scheme 2).

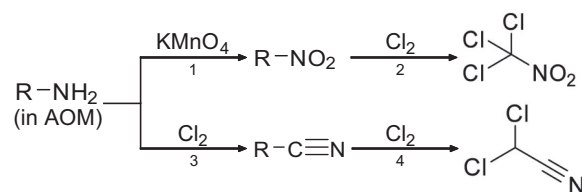
Similar to DCAN, the impact of permanganate preoxidation on the formation of TCNM also differed between chlorination and chloramination of AOM. While permanganate increased the yield of TCNM during chlorination (Fig. 1d), the yield of TCNM was comparable to the control except when we used 3 mg/L permanganate (i.e., the yield increased by  $170 \pm 30\%$  relative to the control, Fig. 3d). Our results indicate that permanganate at an intermediate concentration (i.e., 3 mg/L) oxidizes organic amines to organic nitro compounds that are reactive with monochloramine. However, these precursors may also contain other organic moieties (e.g., aromatic groups) that further react with permanganate (Laszakovits et al., 2020). Therefore, a higher

permanganate concentration (i.e., 5 mg/L) may also oxidize these TCNM precursors to become less reactive with monochloramine. Compared to AOM, the yield of TCNM during chloramination of NOM was either unchanged or slightly decreased (Fig. 3h). The increased formation of TCNM from only AOM suggests that organic amines from AOM are more susceptible than NOM to react with permanganate to produce organic nitro compounds that go on to generate TCNM.

### 3.4. Impact of preoxidation on the toxicity of treated water

Because permanganate preoxidation had different effects on the formation of each DBP, we next calculated the summed toxicity associated with detected DBPs (Szczuka et al., 2017; Wagner and Plewa, 2017; Zeng et al., 2016) to estimate the overall impact of preoxidation on the toxicity of treated water. After permanganate preoxidation, we found that subsequent chlorination led to weighted toxicity that was an order of magnitude higher than subsequent chloramination, which was attributed to the orders of magnitude higher concentrations of DBPs generated by chlorination (Fig. 1) than chloramination (Fig. 3). In addition, although DCAN occurred at 1–2 orders of magnitude lower concentrations than the most abundant DBP TCM, it contributed to ~60–100% of the overall toxicity in all solutions (Fig. 4). This observation was consistent with previous studies that identified haloacetonitriles as the primary contributors to the toxicity of treated AOM and NOM among DBPs considered across these studies (Kralles et al., 2020; Lau et al., 2020; Muellner et al., 2007; Plewa et al., 2017).

Because DCAN was found to be the primary toxicity driver from AOM, the changes in the overall toxicity were most closely related to the changes in DCAN concentrations. For example, permanganate preoxidation decreased the formation of DCAN from chlorination of AOM (relative to the control, Fig. 1c), leading to decreased toxicity relative to the control (Fig. 4a). However, as the formation of DCAN during the chloramination of AOM increased (Fig. 2c), the estimated toxicity increased (Fig. 4b). Although permanganate preoxidation increased the



**Scheme 1.** Formation pathways of dichloroacetonitrile (DCAN) and trichloronitromethane (TCNM) from organic amines of AOM during permanganate preoxidation and chlorination. Oxidation of organic amines by permanganate to form organic nitro compounds (step 1) (Laszakovits et al., 2022; Li et al., 2021; Wei, 1965), followed by formation of TCNM during chlorination (step 2) (Fang et al., 2010b; Shah and Mitch, 2012). Transformation of organic amines to form organic nitrile compounds during chlorination (step 3) (Fang et al., 2010b; Shah and Mitch, 2012), followed by formation of DCAN (step 4) (Fang et al., 2010b; Shah and Mitch, 2012).

toxicity from chloramination of AOM at all permanganate doses relative to the control, the estimated toxicity after chloramination of AOM was decreased as the initial permanganate concentration was increased from 1 to 5 mg/L (Fig. 4b). Therefore, higher doses of permanganate reduced the toxicity after chloramination relative to lower doses.

Our results showed that permanganate preoxidation decreased the estimated toxicity from NOM after chlorination or chloramination (Fig. 4c-d). Similar to AOM, DCAN was a primary contributor to the toxicity from NOM. However, because chlorination of NOM also yielded greater TCM and less DCAN than AOM, TCM also contributed to a larger portion of the overall toxicity after chlorination of NOM (i.e., 30–40%, Fig. 4c) than AOM (i.e., ~10%, Fig. 4a). As permanganate preoxidation decreased the formation of both TCM and DCAN, the estimated toxicity after chlorination of NOM was decreased (Fig. 4c).

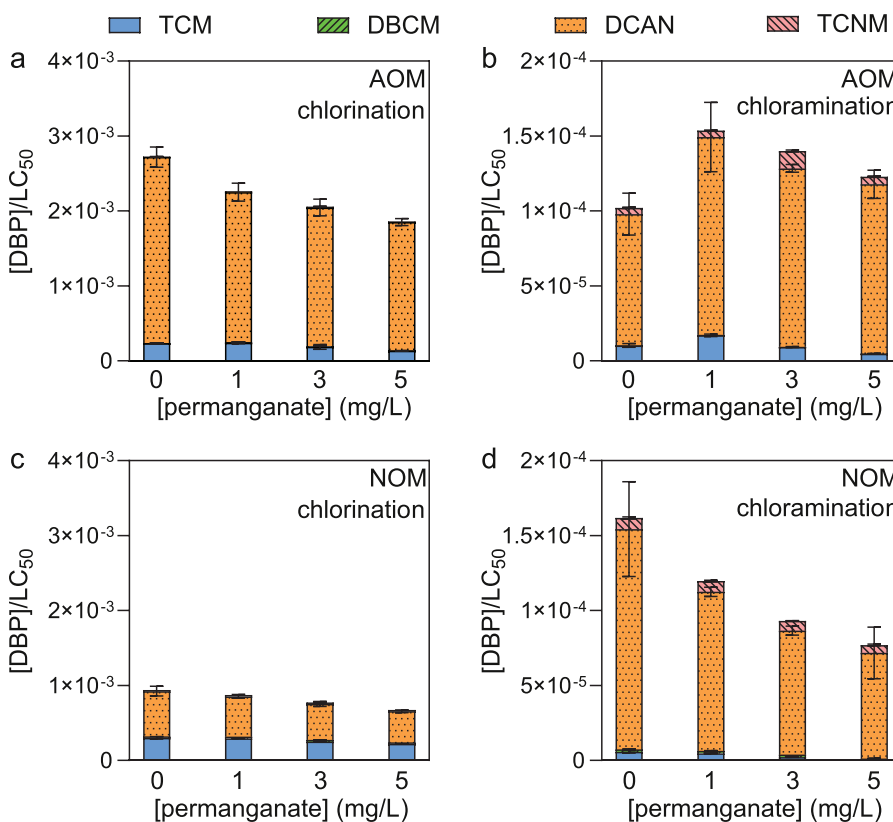
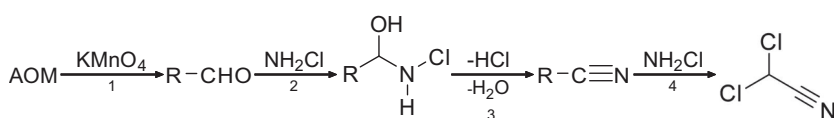


**Fig. 4.** The impact of permanganate preoxidation on summed toxicity associated with detected DBPs (Szczuka et al., 2017; Wagner and Plewa, 2017; Zeng et al., 2016) from (a-b) AOM or (c-d) NOM. All solutions were prepared in headspace-free amber vials initially containing 5 mg-C/L AOM (a-b) or 3 mg-C/L NOM (c-d) and 10 mM phosphate buffer (pH 7). After 3 d, 15 mg/L chlorine (as Cl<sub>2</sub>, a and c) or 4 mg/L monochloramine (as Cl<sub>2</sub>, b and d) was added as the disinfectant to all solutions. Error bars represent the standard deviation of triplicate experiments.



pounds to produce N-chloroaminomethanol (step 2) (Pedersen et al., 1999; Shah and Mitch, 2012); hydrochloric acid and dehydration (step 3) (Fang et al., 2010b; Pedersen et al., 1999; Shah and Mitch, 2012); and transformation of organic nitrile compounds to DCAN during chloramination (step 4) (Fang et al., 2010b; Pedersen et al., 1999; Shah and Mitch, 2012).

#### 4. Conclusions

Our work demonstrated that, while permanganate preoxidation tended to decrease DBP formation from NOM, permanganate preoxidation increased the formation of certain DBPs during chlorination and chloramination of AOM. The following conclusions were drawn:

- Among DBPs considered in our study, DCAN was the primary toxicity driver in AOM-impacted water, suggesting that the formation of DCAN must be controlled to mitigate the toxicity of drinking water during HABs. While permanganate preoxidation consistently decreased the formation of DCAN during both chlorination and chloramination of NOM, its effect on DCAN formation from AOM was variable.
- When followed by chlorination, permanganate preoxidation decreased DCAN formation by up to 40%, which we attributed to oxidation of organic amine moieties under excess permanganate conditions that reduces their availability to form organic nitrile compounds during chlorination (Scheme 1).
- In contrast to chlorination, DCAN formation during chloramination was increased by 30–50% when permanganate preoxidation was applied; this distinction may relate to the ability of monochloramine to contribute its nitrogen when reacting with non-nitrogenous precursors (i.e., organic aldehydes) generated during permanganate preoxidation of AOM that can then become new precursors of DCAN (Scheme 2).
- Beyond DCAN, permanganate preoxidation also altered the formation of other DBPs, most notably by increasing the formation of TCNM from AOM during both chlorination and chloramination at certain doses. Like DCAN, TCNM formation might also be related to the reaction of permanganate with organic amines, which were oxidized to nitro groups that led to increased TCNM formation (Scheme 1).
- In addition to TCNM, permanganate preoxidation also increased the formation of DCBM – particularly in contrast to the decreased formation of its chlorinated analogue, TCM – during both chlorination and chloramination of AOM.
- Overall, our work indicated that permanganate increased the formation of some DBPs during HABs, which will be specifically applicable when permanganate is applied at sufficient doses to lyse algal cells and release AOM.

#### Declaration of Competing Interest

All authors declare that they have no competing financial interest.

#### Data availability

Data will be made available on request.

#### Acknowledgments

This work is supported by the U.S. Geological Survey (G16AP00066, Project 00069900) and National Science Foundation (ECO-CBET 2033714). We thank Dr. Daniel Giammar and Dr. Fuzhong Zhang for

**Scheme 2.** Formation pathway of dichloroacetonitrile (DCAN) during permanganate preoxidation and chloramination of AOM. Oxidation of AOM to organic aldehyde compounds (step 1) (Li et al., 2021; Rawalay and Shechter, 1967; Shaabani et al., 2005; Shechter and Rawalay, 1964; Wei, 1965); contribution of monochloramine nitrogen to organic aldehyde compounds to formation of organic nitrile compounds through elimination of HCl (step 2) (Pedersen et al., 1999; Shah and Mitch, 2012); and transformation of organic nitrile compounds to DCAN during chloramination (step 3) (Fang et al., 2010b; Pedersen et al., 1999; Shah and Mitch, 2012).

access to some of the chemicals used in this work and Dr. Yinjie Tang for access to the UV-vis spectrophotometer.

#### Supplementary materials

Supplementary material associated with this article can be found, in the online version, at [doi:10.1016/j.watres.2023.119691](https://doi.org/10.1016/j.watres.2023.119691).

#### References

Broadwater, M.A., Swanson, T.L., Sivey, J.D., 2018. Emerging investigators series: comparing the inherent reactivity of often-overlooked aqueous chlorinating and brominating agents toward salicylic acid. *Environ. Sci. Water Res. Technol.* 4, 369–384. <https://doi.org/10.1039/c7ew00491e>.

Chen, J.J., Yeh, H.H., 2005. The mechanisms of potassium permanganate on algae removal. *Water Res.* 39, 4420–4428. <https://doi.org/10.1016/j.watres.2005.08.032>.

Chien, I.C., Wu, S.P., Ke, H.C., Lo, S.L., Tung, H.H., 2018. Comparing ozonation and biofiltration treatment of source water with high cyanobacteria-derived organic matter: the case of a water treatment plant followed by a small-scale water distribution system. *Int. J. Environ. Res. Public Health* 15, 2633. <https://doi.org/10.3390/ijerph15122633>.

Dong, F., Lin, Q., Li, C., He, G., Deng, Y., 2021. Impacts of pre-oxidation on the formation of disinfection byproducts from algal organic matter in subsequent chlor(am)ination: a review. *Sci. Total Environ.* 754, 141955. <https://doi.org/10.1016/j.scitotenv.2020.141955>.

Fan, J., Ho, L., Hobson, P., Brookes, J., 2013. Evaluating the effectiveness of copper sulphate, chlorine, potassium permanganate, hydrogen peroxide and ozone on cyanobacterial cell integrity. *Water Res.* 47, 5153–5164. <https://doi.org/10.1016/j.watres.2013.05.057>.

Fang, J., Ma, J., Yang, X., Shang, C., 2010a. Formation of carbonaceous and nitrogenous disinfection by-products from the chlorination of *Microcystis aeruginosa*. *Water Res.* 44, 1934–1940. <https://doi.org/10.1016/j.watres.2009.11.046>.

Fang, J., Yang, X., Ma, J., Shang, C., Zhao, Q., 2010b. Characterization of algal organic matter and formation of DBPs from chlor(am)ination. *Water Res.* 44, 5897–5906. <https://doi.org/10.1016/j.watres.2010.07.009>.

Gallard, H., Von Gunten, U., 2002. Chlorination of natural organic matter: kinetics of chlorination and of THM formation. *Water Res.* 36, 65–74. [https://doi.org/10.1016/S0043-1354\(01\)00187-7](https://doi.org/10.1016/S0043-1354(01)00187-7).

Greenstein, K.E., Zamyadi, A., Glover, C.M., Adams, C., Rosenfeldt, E., Wert, E.C., 2020. Delayed release of intracellular microcystin following partial oxidation of cultured and naturally occurring cyanobacteria. *Toxins* 12, 335. <https://doi.org/10.3390/toxins12050335>.

Gu, X., Zhai, H., Zhou, Y., 2020. Formation of disinfection byproducts from algal organic matter exposed to monochloramine: effects of monochloramine dosages, pH, and bromide concentrations. *Water Air Soil Pollut.* 231, 207. <https://doi.org/10.1007/s11270-020-04597-9>.

Hallegraef, G.M., Enevoldsen, H., Zingone, A., 2021a. Global harmful algal bloom status reporting. *Harmful Algae* 102, 101992. <https://doi.org/10.1016/j.hal.2021.101992>.

Hallegraef, G.M., Anderson, D.M., Belin, C., Bottekin, M.-Y.D., Bresman, E., Chinain, M., Enevoldsen, H., Iwataki, M., Karlson, B., McKenzie, C.H., Sunesen, I., Pitcher, G.C., Provoost, P., Richardson, A., Schweibold, L., Tester, P.A., Trainer, V.L., Yñiguez, A. T., Zingone, A., 2021b. Perceived global increase in algal blooms is attributable to intensified monitoring and emerging bloom impacts. *Commun. Earth Environ.* 2, 117. <https://doi.org/10.1038/s43247-021-00178-8>.

He, S., Ren, N., 2022. Permanganate/bisulfite pre-oxidation of natural organic matter enhances nitrogenous disinfection by-products formation during subsequent chlorination. *Water (Basel)* 14, 507. <https://doi.org/10.3390/w14030507>.

Heeb, M.B., Criquet, J., Zimmermann-Steffens, S.G., Von Gunten, U., 2014. Oxidative treatment of bromide-containing waters: formation of bromine and its reactions with inorganic and organic compounds—a critical review. *Water Res.* 48, 15–42. <https://doi.org/10.1016/j.watres.2013.08.030>.

Hidayah, E.N., Yeh, H.H., 2018. Effect of permanganate preoxidation to natural organic matter and disinfection by-products formation potential removal. *J. Phys. Conf. Ser.* 953, 012218. <https://doi.org/10.1088/1742-6596/953/1/012218>.

Hu, J., Chu, W., Sui, M., Xu, B., Gao, N., Ding, S., 2018. Comparison of drinking water treatment processes combinations for the minimization of subsequent disinfection by-products formation during chlorination and chloramination. *Chem. Eng. J.* 335, 352–361. <https://doi.org/10.1016/j.cej.2017.10.144>.

Hua, G., Reckhow, D.A., 2008. DBP formation during chlorination and chloramination: Effect of reaction time, pH, dosage, and temperature. *J. Am. Water Works Assoc.* 100, 82–95. <https://doi.org/10.1002/j.1551-8833.2008.tb09702.x>.

Hua, G., Reckhow, D.A., 2007. Comparison of disinfection byproduct formation from chlorine and alternative disinfectants. *Water Res.* 41, 1667–1678. <https://doi.org/10.1016/j.watres.2007.01.032>.

Hua, G., Reckhow, D.A., Abusallout, I., 2015. Correlation between SUVA and DBP formation during chlorination and chloramination of NOM fractions from different sources. *Chemosphere* 130, 82–89. <https://doi.org/10.1016/j.chemosphere.2015.03.039>.

Hua, L.C., Lin, J.L., Chen, P.C., Huang, C., 2017. Chemical structures of extra- and intra-cellular allogenetic organic matters as precursors to the formation of carbonaceous disinfection byproducts. *Chem. Eng. J.* 328, 1022–1030. <https://doi.org/10.1016/j.cej.2017.07.123>.

Huang, H., Chen, B.Y., Zhu, Z.R., 2017. Formation and speciation of haloacetamides and haloacetonitriles for chlorination, chloramination, and chlorination followed by chloramination. *Chemosphere* 166, 126–134. <https://doi.org/10.1016/j.chemosphere.2016.09.047>.

Hudnell, H.K., 2010. The state of U.S. freshwater harmful algal blooms assessments, policy and legislation. *Toxicon* 55, 1024–1034. <https://doi.org/10.1016/j.toxicon.2009.07.021>.

Hureiki, L., Croué, J.P., Legube, B., Doré, M., 1998. Ozonation of amino acids: ozone demand and aldehyde formation. *Ozone Sci. Eng.* 20, 381–402. <https://doi.org/10.1080/01919519809480349>.

Jia, A., Wu, C., Duan, Y., 2016. Precursors and factors affecting formation of haloacetonitriles and chloropicrin during chlor(am)ination of nitrogenous organic compounds in drinking water. *J. Hazard. Mater.* 308, 411–418. <https://doi.org/10.1016/j.jhazmat.2016.01.037>.

Jiang, Y., Goodwill, J.E., Tobiason, J.E., Reckhow, D.A., 2019. Comparison of ferrate and ozone pre-oxidation on disinfection byproduct formation from chlorination and chloramination. *Water Res.* 156, 110–124. <https://doi.org/10.1016/j.watres.2019.02.051>.

Jiang, Y., Goodwill, J.E., Tobiason, J.E., Reckhow, D.A., 2016. Comparison of the effects of ferrate, ozone, and permanganate pre-oxidation on disinfection byproduct formation from chlorination. *ACS Symp. Ser.* 1238, 421–437. <https://doi.org/10.1021/bk-2016-1238.ch016>.

Kralles, Z.T., Ikuma, K., Dai, N., 2020. Assessing disinfection byproduct risks for algal impacted surface waters and the effects of peracetic acid pre-oxidation. *Environ. Sci. Water Res. Technol.* 6, 2365–2381. <https://doi.org/10.1039/d0ew00237b>.

Kumar, K., Margerum, D.W., 1987. Kinetics and mechanism of general-acid-assisted oxidation of bromide by hypochlorite and hypochlorous acid. *Inorg. Chem.* 26, 2706–2711. <https://doi.org/10.1021/ic00263a030>.

Laszakovits, J.R., Kerr, A., Mackay, A.A., 2022. Permanganate oxidation of organic contaminants and model compounds. *Environ. Sci. Technol.* 56, 4728–4748. <https://doi.org/10.1021/acs.est.1c03621>.

Laszakovits, J.R., Somogyi, A., MacKay, A.A., 2020. Chemical alterations of dissolved organic matter by permanganate oxidation. *Environ. Sci. Technol.* 54, 3256–3266. <https://doi.org/10.1021/acs.est.9b06675>.

Lau, S.S., Wei, X., Bokenkamp, K., Wagner, E.D., Plewa, M.J., Mitch, W.A., 2020. Assessing additivity of cytotoxicity associated with disinfection byproducts in potable reuse and conventional drinking waters. *Environ. Sci. Technol.* 54, 5729–5736. <https://doi.org/10.1021/acs.est.0c00958>.

Li, J., Pang, S.Y., Wang, Z., Guo, Q., Duan, J., Sun, S., Wang, L., Cao, Y., Jiang, J., 2021. Oxidative transformation of emerging organic contaminants by aqueous permanganate: kinetics, products, toxicity changes, and effects of manganese products. *Water Res.* 203, 117513. <https://doi.org/10.1016/j.watres.2021.117513>.

Li, L., Gao, N., Deng, Y., Yao, J., Zhang, K., 2012. Characterization of intracellular & extracellular algae organic matters (AOM) of *Microcystis aeruginosa* and formation of AOM-associated disinfection byproducts and odor & taste compounds. *Water Res.* 46, 1233–1240. <https://doi.org/10.1016/j.watres.2011.12.026>.

Liang, L., Singer, P.C., 2003. Factors influencing the formation and relative distribution of haloacetic acids and trihalomethanes in drinking water. *Environ. Sci. Technol.* 37, 2920–2928. <https://doi.org/10.1021/es026230q>.

Lu, J., Zhang, T., Ma, J., Chen, Z., 2009. Evaluation of disinfection by-products formation during chlorination and chloramination of dissolved natural organic matter fractions isolated from a filtered river water. *J. Hazard. Mater.* 162, 140–145. <https://doi.org/10.1016/j.jhazmat.2008.05.058>.

McCurry, D.L., Quay, A.N., Mitch, W.A., 2016. Ozone promotes chloropicrin formation by oxidizing amines to nitro compounds. *Environ. Sci. Technol.* 50, 1209–1217. <https://doi.org/10.1021/acs.est.5b04282>.

McKenna, E., Thompson, K.A., Taylor-Edmonds, L., McCurry, D.L., Hanigan, D., 2020. Summation of disinfection by-product CHO cell relative toxicity indices: sampling bias, uncertainty, and a path forward. *Environ. Sci. Process. Impacts* 22, 708–718. <https://doi.org/10.1039/c9em00468h>.

Muellner, M.G., Wagner, E.D., Mccalla, K., Richardson, S.D., Woo, Y.T., Plewa, M.J., 2007. Haloacetonitriles vs. regulated haloacetic acids: are nitrogen-containing DBPs more toxic? *Environ. Sci. Technol.* 41, 645–651. <https://doi.org/10.1021/es0617441>.

Naceradska, J., Pivokonsky, M., Pivokonska, L., Baresova, M., Henderson, R.K., Zamyadi, A., Janda, V., 2017. The impact of pre-oxidation with potassium permanganate on cyanobacterial organic matter removal by coagulation. *Water Res.* 114, 42–49. <https://doi.org/10.1016/j.watres.2017.02.029>.

Novoa, A.F., Vrouwenvelder, J.S., Fortunato, L., 2021. Membrane fouling in algal separation processes: a review of influencing factors and mechanisms. *Front. Chem. Eng.* 3, 1–18. <https://doi.org/10.3389/fceng.2021.687422>.

Pedersen, E.J., Urbansky, E.T., Mariñas, B.J., Margerum, D.W., 1999. Formation of cyanogen chloride from the reaction of monochloramine with formaldehyde. *Environ. Sci. Technol.* 33, 4239–4249. <https://doi.org/10.1021/es990153q>.

Perez-Benito, J.F., 2009. Autocatalytic reaction pathway on manganese dioxide colloidal particles in the permanganate oxidation of glycine. *J. Phys. Chem. C* 113, 15982–15991. <https://doi.org/10.1021/jp9014178>.

Piezer, K., Li, L., Jeon, Y., Kadudula, A., Seo, Y., 2021. The application of potassium permanganate to treat cyanobacteria-laden water: a review. *Process Saf. Environ. Prot.* 148, 400–414. <https://doi.org/10.1016/j.psep.2020.09.058>.

Plewa, M.J., Wagner, E.D., Richardson, S.D., 2017. TIC-Tox: a preliminary discussion on identifying the forcing agents of DBP-mediated toxicity of disinfected water. *J. Environ. Sci.* 58, 208–216. <https://doi.org/10.1016/j.jes.2017.04.014>.

Plummer, J.D., Edzwald, J.K., 2001. Effect of ozone on algae as precursors for trihalomethane and haloacetic acid production. *Environ. Sci. Technol.* 35, 3661–3668. <https://doi.org/10.1021/es0106570>.

Qi, J., Ma, B., Miao, S., Liu, R., Hu, C., Qu, J., 2021. Pre-oxidation enhanced cyanobacteria removal in drinking water treatment: a review. *J. Environ. Sci.* 110, 160–168. <https://doi.org/10.1016/j.jes.2021.03.040>.

Rawalay, S.S., Shechter, H., 1967. Oxidation of primary, secondary, and tertiary amines with neutral permanganate. a simple method for degrading amines to aldehydes and ketones. *J. Org. Chem.* 32, 3129–3131. <https://doi.org/10.1021/jo01285a042>.

Reckhow, D.A., Singer, P.C., Malcolm, R.L., 1990. Chlorination of humic materials: byproduct formation and chemical interpretations. *Environ. Sci. Technol.* 24, 1655–1664. <https://doi.org/10.1021/es00081a005>.

Roberts, V.A., Vigar, M., Backer, L., Veytsel, G.E., Hilborn, E.D., Hamelin, E.I., Vanden Esschert, K.L., Lively, J.Y., Cope, J.R., Hlavsa, M.C., Yoder, J.S., 2020. Surveillance for harmful algal bloom events and associated human and animal illnesses — one health harmful algal bloom system, United States, 2016–2018. *MMWR Morb. Mortal. Wkly. Rep.* 69, 1889–1894. <https://doi.org/10.15585/mmwr.mm6950a2>.

Rodríguez, E., Majado, M.E., Meriluoto, J., Acero, J.L., 2007a. Oxidation of microcystins by permanganate: reaction kinetics and implications for water treatment. *Water Res.* 41, 102–110. <https://doi.org/10.1016/j.watres.2006.10.004>.

Rodríguez, E., Onstad, G.D., Kull, T.P.J., Metcalf, J.S., Acero, J.L., von Gunten, U., 2007b. Oxidative elimination of cyanotoxins: comparison of ozone, chlorine, chlorine dioxide and permanganate. *Water Res.* 41, 3381–3393. <https://doi.org/10.1016/j.watres.2007.03.033>.

Rougé, V., Von Gunten, U., Allard, S., 2020a. Efficiency of pre-oxidation of natural organic matter for the mitigation of disinfection byproducts: electron donating capacity and UV absorbance as surrogate parameters. *Water Res.* 187, 116418. <https://doi.org/10.1016/j.watres.2020.116418>.

Rougé, V., Von Gunten, U., Lafont De Sentenac, M., Massi, M., Wright, P.J., Croué, J.P., Allard, S., 2020b. Comparison of the impact of ozone, chlorine dioxide, ferrate and permanganate pre-oxidation on organic disinfection byproduct formation during post-chlorination. *Environ. Sci. Water Res. Technol.* 6, 2382–2395. <https://doi.org/10.1039/d0ew00411a>.

Shaabani, A., Tavasoli-Rad, F., Lee, D.G., 2005. Potassium permanganate oxidation of organic compounds. *Synth. Commun.* 35, 571–580. <https://doi.org/10.1081/SCC-200049792>.

Shah, A.D., Mitch, W.A., 2012. Halonitroalkanes, halonitriles, haloamides, and N-nitrosamines: a critical review of nitrogenous disinfection byproduct formation pathways. *Environ. Sci. Technol.* 46, 119–131. <https://doi.org/10.1021/es203312s>.

Shechter, H., Rawalay, S.S., 1964. Oxidation of primary, secondary, and tertiary amines with neutral potassium permanganate. II. *J. Am. Chem. Soc.* 86, 1706–1709. <https://doi.org/10.1021/ja01063a013>.

Sheng, D., Bu, L., Zhu, S., Wu, Y., Wang, J., Li, N., Zhou, S., 2022. Impact of pre-oxidation on the formation of byproducts in algae-laden water disinfection: insights from fluorescent and molecular weight. *J. Environ. Sci.* 117, 21–27. <https://doi.org/10.1016/j.jes.2021.12.021>.

Shi, X., Bi, R., Yuan, B., Liao, X., Zhou, Z., Li, F., Sun, W., 2019. A comparison of trichloromethane formation from two algae species during two pre-oxidation-coagulation-chlorination processes. *Sci. Total Environ.* 656, 1063–1070. <https://doi.org/10.1016/j.scitotenv.2018.11.461>.

Sivey, J.D., Arey, J.S., Tentscher, P.R., Roberts, A.L., 2013. Reactivity of BrCl, Br<sub>2</sub>, BrOCl, Br<sub>2</sub>O and HOBr toward dimethenamid in solutions of bromide + aqueous free chlorine. *Environ. Sci. Technol.* 47, 8990. <https://doi.org/10.1021/es402917a>.

Sivey, J.D., Bickley, M.A., Victor, D.A., 2015. Contributions of BrCl, Br<sub>2</sub>, BrOCl, Br<sub>2</sub>O, and HOBr to regiospecific bromination rates of anisole and bromoanisoles in aqueous solution. *Environ. Sci. Technol.* 49, 4937–4945. <https://doi.org/10.1021/acs.est.5b00205>.

Szczuka, A., Parker, K.M., Harvey, C., Hayes, E., Vengosh, A., Mitch, W.A., 2017. Regulated and unregulated halogenated disinfection byproduct formation from chlorination of saline groundwater. *Water Res.* 122, 633–644. <https://doi.org/10.1016/j.watres.2017.06.028>.

U.S. EPA, 1999. Alternative Disinfectants and Oxidants Guidance Manual (No. EPA 815-R-99-014). U.S. EPA Office of Water: Washington, DC.

Wagner, E.D., Plewa, M.J., 2017. CHO cell cytotoxicity and genotoxicity analyses of disinfection by-products: an updated review. *J. Environ. Sci.* 58, 64–76. <https://doi.org/10.1016/j.jes.2017.04.021>.

Waldemer, R.H., Tratnyek, P.G., 2006. Kinetics of contaminant degradation by permanganate. *Environ. Sci. Technol.* 40, 1055–1061. <https://doi.org/10.1021/es051330s>.

Wang, A., Lin, C., Shen, Z., Liu, Z., Xu, H., Cheng, J., Wen, X., 2020. Effects of pre-oxidation on haloacetonitrile and trichloronitromethane formation during subsequent chlorination of nitrogenous organic compounds. *Int. J. Environ. Res. Public Health* 17, 1046. <https://doi.org/10.3390/ijerph17031046>.

Wang, R., Ji, M., Zhai, H., Liang, Y., 2020. Electron donating capacities of DOM model compounds and their relationships with chlorine demand, byproduct formation, and other properties in chlorination. *Chemosphere* 261, 127764. <https://doi.org/10.1016/j.chemosphere.2020.127764>.

Wei, M., 1965. Mechanism of Permanganate Oxidation of Aliphatic Amines (Doctoral Dissertation). The University of British Columbia, Vancouver, BC. <https://doi.org/10.14288/1.0062255>.

Wert, E.C., Rosario-Ortiz, F.L., 2013. Intracellular organic matter from cyanobacteria as a precursor for carbonaceous and nitrogenous disinfection byproducts. *Environ. Sci. Technol.* 47, 6332–6340. <https://doi.org/10.1021/es400834k>.

Xie, P., Chen, Y., Ma, J., Zhang, X., Zou, J., Wang, Z., 2016. A mini review of preoxidation to improve coagulation. *Chemosphere* 155, 550–563. <https://doi.org/10.1016/j.chemosphere.2016.04.003>.

Xie, P., Ma, J., Fang, J., Guan, Y., Yue, S., Li, X., Chen, L., 2013. Comparison of permanganate preoxidation and preozonation on algae containing water: cell integrity, characteristics, and chlorinated disinfection byproduct formation. *Environ. Sci. Technol.* 47, 14051–14061. <https://doi.org/10.1021/es4027024>.

Xu, B., Ye, T., Li, D.P., Hu, C.Y., Lin, Y.L., Xia, S.J., Tian, F.X., Gao, N.Y., 2011. Measurement of dissolved organic nitrogen in a drinking water treatment plant: size fraction, fate, and relation to water quality parameters. *Sci. Total Environ.* 409, 1116–1122. <https://doi.org/10.1016/j.scitotenv.2010.12.016>.

Yang, X., Guo, W., Lee, W., 2013. Formation of disinfection byproducts upon chlorine dioxide preoxidation followed by chlorination or chloramination of natural organic matter. *Chemosphere* 91, 1477–1485. <https://doi.org/10.1016/j.chemosphere.2012.12.014>.

Yang, X., Guo, W., Shen, Q., 2011. Formation of disinfection byproducts from chlor(am)ination of algal organic matter. *J. Hazard. Mater.* 197, 378–388. <https://doi.org/10.1016/j.jhazmat.2011.09.098>.

Yang, X., Shen, Q., Guo, W., Peng, J., Liang, Y., 2012. Precursors and nitrogen origins of trichloronitromethane and dichloroacetonitrile during chlorination/chloramination. *Chemosphere* 88, 25–32. <https://doi.org/10.1016/j.chemosphere.2012.02.035>.

Zeng, T., Plewa, M.J., Mitch, W.A., 2016. N-Nitrosamines and halogenated disinfection byproducts in U.S. full advanced treatment trains for potable reuse. *Water Res.* 101, 176–186. <https://doi.org/10.1016/j.watres.2016.03.062>.

Zhang, Q., Liu, B., Liu, Y., 2014. Effect of ozone on algal organic matters as precursors for disinfection by-products production. *Environ. Technol.* 35, 1753–1759. <https://doi.org/10.1080/09593330.2014.881422>.

Zhang, T.Y., Lin, Y.L., Xu, B., Cheng, T., Xia, S.J., Chu, W.H., Gao, N.Y., 2016. Formation of organic chloramines during chlor(am)ination and UV/chlor(am)ination of algae organic matter in drinking water. *Water Res.* 103, 189–196. <https://doi.org/10.1016/j.watres.2016.07.036>.

Zhang, X., Chen, Z., Shen, J., Zhao, S., Kang, J., Chu, W., Zhou, Y., Wang, B., 2020. Formation and interdependence of disinfection byproducts during chlorination of natural organic matter in a conventional drinking water treatment plant. *Chemosphere* 242, 125227. <https://doi.org/10.1016/j.chemosphere.2019.125227>.

Zhou, S., Shao, Y., Gao, N., Li, L., Deng, J., Zhu, M., Zhu, S., 2014. Effect of chlorine dioxide on cyanobacterial cell integrity, toxin degradation and disinfection by-product formation. *Sci. Total Environ.* 482–483, 208–213. <https://doi.org/10.1016/j.scitotenv.2014.03.007>.

Zhou, S., Zhu, S., Shao, Y., Gao, N., 2015. Characteristics of C-, N-DBPs formation from algal organic matter: role of molecular weight fractions and impacts of pre-ozonation. *Water Res.* 72, 381–390. <https://doi.org/10.1016/j.watres.2014.11.023>.

Zhu, M., Gao, N., Chu, W., Zhou, S., Zhang, Z., Xu, Y., Dai, Q., 2015. Impact of pre-ozonation on disinfection by-product formation and speciation from chlor(am)ination of algal organic matter of *Microcystis aeruginosa*. *Ecotoxicol. Environ. Saf.* 120, 256–262. <https://doi.org/10.1016/j.ecoenv.2015.05.048>.